

# Hybrid Neural Network Methods for Lithology Identification in the Algerian Sahara

S. Chikhi, M. Batouche, and H. Shout

**Abstract**— In this paper, we combine a probabilistic neural method with radial-bias functions in order to construct the lithofacies of the wells DF01, DF02 and DF03 situated in the Triassic province of Algeria (Sahara). Lithofacies is a crucial problem in reservoir characterization. Our objective is to facilitate the experts' work in geological domain and to allow them to obtain quickly the structure and the nature of lands around the drilling. This study intends to design a tool that helps automatic deduction from numerical data. We used a probabilistic formalism to enhance the classification process initiated by a Self-Organized Map procedure. Our system gives lithofacies, from well-log data, of the concerned reservoir wells in an aspect easy to read by a geology expert who identifies the potential for oil production at a given source and so forms the basis for estimating the financial returns and economic benefits.

**Keywords**— Classification, Lithofacies, Probabilistic formalism, Reservoir characterization, Well-log data.

## I. INTRODUCTION

THE prediction of lithofacies is an important issue for many geological and engineering disciplines. Lithofacies that consists of a rock type identification, can be used to correlate many important characteristics of a reservoir. For petroleum reservoir characterization, the primary task is to identify lithofacies of the reservoir rocks.

Generally, one identifies lithofacies by direct observation of underground cores, which are small cylindrical rock samples retrieved from wells at selected well depths. The recuperation of cores is an expensive process and is not always total. It is why a lower-cost method providing similar or higher accuracy is desirable. In this paper, we use differed well logging which consists on a set of records of a digital measurements obtained along the depth of the oil and gas wells. This method provides indirect information about the subsurface and is far less expensive. Our purpose is to describe an automated method, based on neural networks, of predicting reservoir rock characteristics from differed well-log data. In an attempt to solve such reservoir characterization problems and using differed well logging measurements, some researchers in

geosciences have recently employed statistical methods ([7], [24], [26]) and artificial neural networks (ANNs) ([16], [29]). Applications of ANNs such permeability prediction modeling and reservoir parameter estimation using a hybrid neural network ([5], [23]), have demonstrated their effectiveness in prediction, estimation and characterization.

However, ANNs have several significant disadvantages. First, convergence during training is slow and there is no guarantee of reaching the user-defined acceptable error range. Second, when test data are located outside the training data range, ANN cannot classify them; thus, the discriminating ability is not assured. ANNs adequately deal with well-bounded and stable problems, because training sets may cover the entire expected input space. Unfortunately, in reservoir characterization problems, variables commonly are neither well bounded nor stable. New lithofacies and new values of important rock properties are often encountered.

We use a PRSOM neural network, which is a probabilistic variant of the self-organizing map of Kohonen [20] to propose a logfacies-recognizer system (*geonal*). The global conception scheme of the *geonal* system is described in fig. 1. PRSOM is an unsupervised learning algorithm, which adapt the map to a set of learning samples. This algorithm allows realizing a partition of the data space, with each subset associated to a neuron of the map. PRSOM is a probabilistic model, which associates to a neuron  $c$  of the map a spherical Gaussian density function  $f_c$ , it approximates the data's density distribution using a mixture of normal distributions.

## II. LOGFACIES AND LITHOFACIES

Well-log measurements can be classified into logfacies. Logfacies are defined as the collective set of log responses, reflecting both the rock and fluid properties, allowing discrimination among beds or sedimentary units. Logfacies commonly correspond to lithofacies when they are calibrated with core descriptions. Thus, logfacies may be constructed as surrogates for lithofacies. Well-log data ([2], [14], [24]) are records of geological properties of subsurface rock formations at depth retrieved by electrical, physical, or radioactive devices. They permit to do several measures. Classifications that learn to identify logfacies can then be used to predict lithofacies in non-cored wells or non-cored intervals in cored wells. Due to the heterogeneous nature of rocks, associating well-log data with lithofacies can be difficult. Carbonate lithofacies identification using log data is more demanding because they can be defined using any set of rock properties.

Manuscript received March 16, 2004.

S. Chikhi is with the LIRE Laboratory Computer Science Department, University of Constantine (phone: +213 3161 4346; fax: +213 3181 8711; e-mail: slchikhi@yahoo.com).

M. Batouche, was with National Polytechnic Institute Lorraine, Nancy, France where he receives his Ph.D. degree in Computer Science. Currently, he is full Professor at Mentouri University of Constantine (e-mail: batouche@wissal.dz)

H. Shout is with the Earth Science Laboratory, Mentouri University of Constantine (shout@wissal.dz).

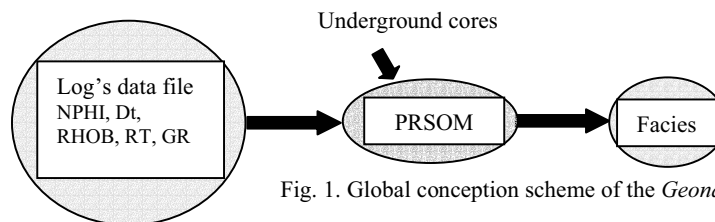


Fig. 1. Global conception scheme of the *Geonal* system

The following well-log data are used in this paper to correlate the lithofacies: Neutron porosity log (NPHI), Sonic log (Dt), Bulk density log (RHOB), Gamma ray log (GR), Deep resistivity (RT). We describe briefly the usefulness of each parameter used in this study for the identification process of rocks.

- Neutron porosity log (NPHI): It measures the rock's reaction to fast neutron bombardment. The unit is dimensionless. The recorded parameter is an index of hydrogen for a given formation of lithology, generally of the limestone (as well as sandstone or dolomite). NPHI is useful mainly for: -lithology identification -Porosity evaluation, and -Differentiation between liquids and gases (in combination with the density).

- Travel time or Sonic log (Dt): The unit is  $\mu\text{s}/\text{ft}$ . It measures the variations of the speed of acoustic wave propagation according to the depth. It must be done in "open" hole, that means before the pose of the protective intubations. It is useful mainly for: -Determination of the porosity in a non-clayey formation, and -Identification of the lithology (in combination with neutron and density).

- Bulk density log (RHOB): The unit is  $\text{g}/\text{cc}$  (grams per cubic centimeter). It measures the bulk density of rock by measuring the bombardment of medium-high energy gamma rays. Densities the most fluently measured evolve between 2 and 3  $\text{g}/\text{cm}^3$ . RHOB is useful mainly for: -Determination of the porosity in zones to hydrocarbons or in formations containing the clay, and -Differentiation between liquids and gases (in combination with Neutron).

- Gamma ray log (GR): The unit is API (American Petroleum Institute). It measures the radioactivity of rocks and is useful mainly for: -Geological correlations, correlations of depths, -Differentiation between clean zones and clayey zones, and -Evaluation of the content in clay of formations.

- Deep resistivity (RT): The unit is ohm. It measures the fluid resistivities at deep vicinity of the wells by using long focusing electrodes and a distant return electrode. The rock resistivity measure is a data of basis of all reservoir evaluation. It is useful mainly for having an idea about: -the quantities of water in the rock therefore the porosity and the saturation of the lithology, -nature and percentage of clay and nature and percentage of mineral, and -texture of the rock (fashion of pore distribution). Therefore the true resistivity of a rock is resulting of the matrix and its content in fluid.

In this study all logs are scaled uniformly between  $-1$  and  $+1$  and results are given in scaled domain. Fig. 2 and 3 show the interaction between logs used respectively in DF02 and by the SOM algorithm. We combine the non-supervised PRSOM algorithm and radial-bias functions to solve problems for which we possess information on the expected result like

DF03 wells. Fig. 4 shows the well logging measurements (logfacies) of DF02.

### III. SUPERVISED AND UNSUPERVISED CLASSIFICATION

Neural networks learning may be broadly grouped as supervised and unsupervised. In supervised learning, the network learns from a training set consisting of inputs and the desired outputs. Learning is accomplished by adjusting the network weights so that the difference between the desired outputs and the network-computed outputs is minimized. BPNs are examples of supervised learning. Unsupervised learning ([9], [15]) requires only input data. During the learning process, the network weights are adjusted so that similar inputs produce similar outputs. Kohonen's self-organizing maps (SOMs) ([18], [20]), and adaptive resonance theory (ART) neural networks ([10], [11]) are examples of unsupervised learning. They extract statistical regularities from the input data automatically rather than using desired outputs to guide the learning processes. Several researchers employed pattern recognition with unsupervised learning neural networks as pattern-recognizers to solve a lithofacies identification problem; e.g., SOMs and ART neural networks ([12], [21]).

### IV. THE SELF-ORGANIZING MAP

To represent the facies of the drilling holes DF02 and DF03, we used a Self-Organizing Map (SOM) ([18][20]). The SOM algorithm realizes a partition of the data space that permits to affect each vector of the data space to a particular neuron on the map. We have used available underground cores (only 503 points) as labels. Then we know the exact nature of the rocks present at the corresponding depth that is used to label each neuron of the map. Thus, the map becomes a classifier. We have used log's data from the well DF02 as a learning base for training the map and then, when the network is stable and represent relatively well the data space, we reuse the map with log's data from well DF03. The best map obtained has a size  $17 \times 5$  (fig. 5) and the lithofacies obtained for DF02 and DF03 are shown in fig. 6 and 7 respectively.

### V. PROBABILISTIC METHOD COMBINED WITH RADIAL-BIAS FUNCTIONS

In this section, we will consider the second algorithm, which is used to obtain a topological map. We already have a good map and we will use this algorithm to refine a map obtained

underground cores and some expertise in our application. Two layers of weights characterize the radial-bias network architecture whereas the PRSOM algorithm turns on a

topological map and performs the first learning phase taking into account a topological structure.

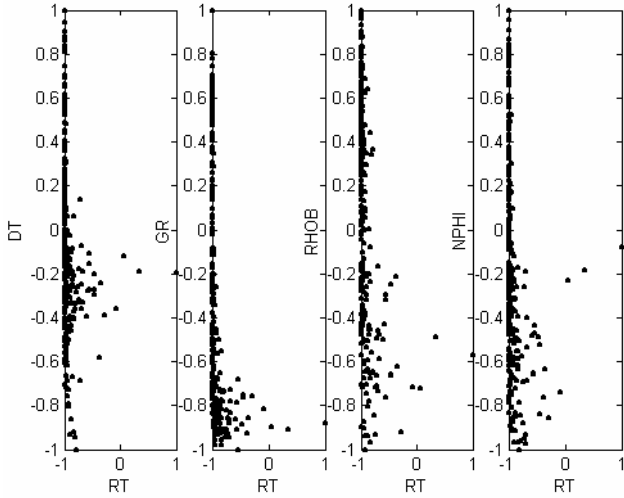


Fig. 2. Crossplots of RT log versus the other logs used for well DF02.

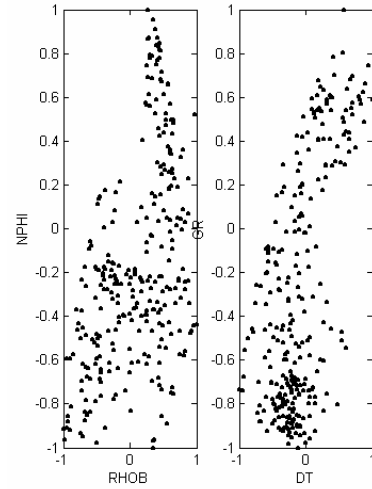


Fig. 3. Crossplots of RHOB and DT versus NPHI and GR logs for well DF03.

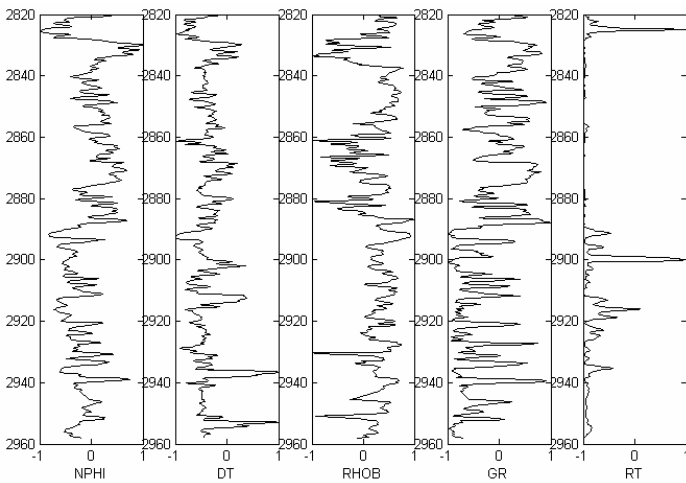


Fig. 4. The logfacies of well DF02

Table I. Legend of rock classes

	Anhydrite salt, gypsum
	Dolomite and dolomitic marl
	Microconglomeratic clay
	Marly limestone
	Red and green clay and argillite
	Quartzite and Quartzite sandstone
	Clay-sandstone
	Chalky or clayey limestone (sandy)
	Micaceous fine sandstone
	Fine to coarse clayey or chalky sand
	Dolomite clayey
	Coarse sandstone

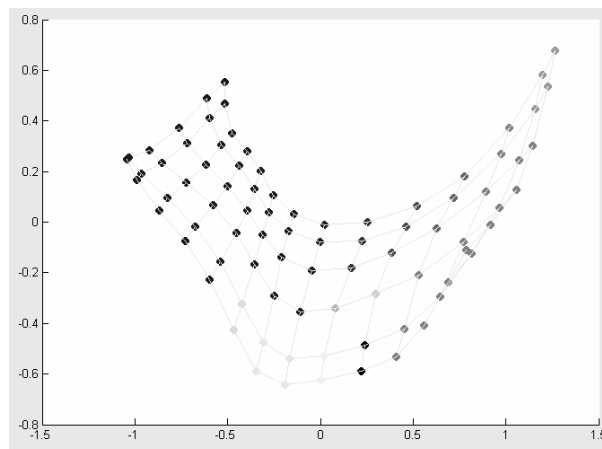


Fig. 5: 3D projection of the best map (17x5) obtained for DF03 (DF02 as learning base)

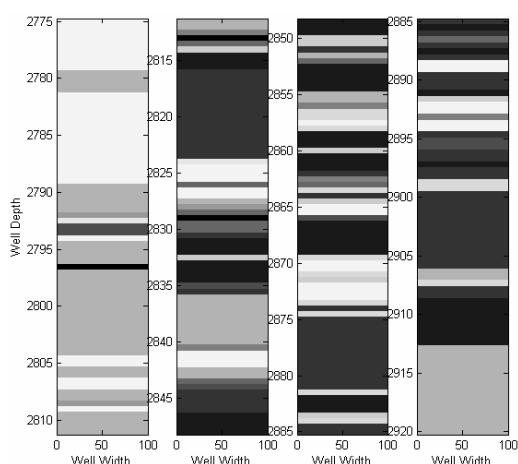


Fig. 6. Lithofacies obtained for DF02 by SOM

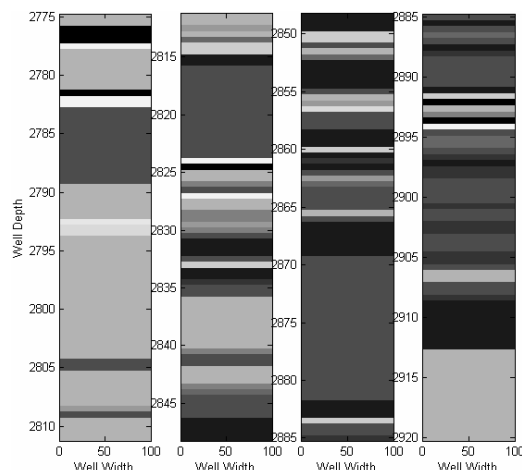


Fig. 7. Lithofacies obtained for DF03 by SOM

### A. Principle of the algorithm

A first version of this algorithm can be found in [12]. PRSOM introduces the notion of density in the topological map. We used data obtained from different observation subsets, each of these subsets being governed by a normal law. Every neuron is the representative of one of these subsets. By the action of the neighborhood a neuron gives account of the subset that it represents, and also of subsets represented by its neighbors. Therefore, each neuron represents a mixture of densities. The data set is discerned as the mixture of the mixture of densities represented by every neuron. A neuron is constituted therefore of 2 elements: a vector of 5 measurements that corresponds to the mean vector and the variance of the normal law that is associated to it ([6], [12], [16]). A neuron defines a gaussian density function. To limit calculations, we consider that the variance is identical in all directions. When an observation is presented to the network, the PRSOM algorithm calculates the activation provoked by this observation in the density function of every neuron of the map. The winning neuron is the one with the strongest activation. All neurons of the map are modified after the presentation of all observations of the

Then each cycle of the algorithm takes place according to the principle shown in table II.

Assessment of the temperature of the cycle: The first operation of the PRSOM training cycle consists in valuing the temperature that will be constant during all the cycle:

$$h(t) = hMax * \left( \frac{hMin}{hMax} \right)^{\frac{1}{cycleMax - t}} \quad (1)$$

Where:

- $h(t)$  : the temperature at the iteration  $t$ ,
- $hMin, hMax$  : the minimum and the maximum temperature, parameters fixed at the beginning of algorithm,
- $N$  : the number of observations in the training set,
- $cycleMax$  : the maximum number of cycles.

*Competition phase driven by radial-bias functions:* All observations of the training set are studied in order to choose

training set (one cycle). To modify parameters of a neuron  $c$ , average and variance, PRSOM takes in account the influence exercised by all observations of the cycle. This influence is pondered by the relation of neighborhood that exists between the winning neuron to which is affected the observation and the neuron  $c$  of which we want to modify parameters. The sum of influences exercised by observations is normalized then by the sum of neighborhood relations binding the neuron  $c$  to the neuron winning every observation. As in the SOM algorithm a "temperature" adjusts the influence of the neighborhood. In PRSOM, this temperature is calculated at the beginning of every cycle, to remain constant during all the cycle.

### B. PRSOM algorithm

First of all, it is necessary to fix some parameters:

- The shape and the dimension of the map,
- The number of neurons on the map,
- The maximum temperature that generates the neighborhood of size maximum
- The minimum temperature that generates the neighborhood of size minimum
- The number of cycles wished.

the winning neuron for each of them. When we present an observation to the network, we look at the behavior of every neuron towards it. For this, we make the hypothesis that the observation is descended of the mixture of densities covered by the neuron. Here, we introduce the radial-bias functions approach, which is to the origin an exact interpolation technique in a multidimensional space. The problem of exact interpolation consists in associating with accurateness to each input vector its output desired value [8]. A certain number of modifications of the exact interpolation procedure gave birth to neuronal models based on radial bias functions and called radial-bias networks. The goal is to get an interpolation function smoothed of which the number of basis functions is not represented anymore by the size of the data set but by a certain number of representatives obtained by a data quantification. If  $k$  is the number of these representatives, for an input  $z$  the output  $y$  of such a network has the form:

$y(z) = \sum_{c=1}^k \lambda_c f_c(z) + \lambda_0$  where  $\{f_c, c=1, \dots, k\}$  is the set of the  $k$

basis functions, and  $\lambda_0$  is a bias. In practice, the most used form of the basis functions is the function:

$$f_c(z) = \exp \left[ -\frac{\|z - W_c\|^2}{2(\sigma_c)^2} \right].$$

We have used a specific radial-bias

$$Rbf(z, c) = \frac{1}{(\sqrt{2\pi} * \sigma_c)^n} * \exp \left[ -0,5 * \sqrt{\sum_{i=1}^n \left[ \frac{z[i] - w_{c[i]}}{\sigma_c} \right]^2} \right] \quad (2)$$

$$g = \chi(x) = \operatorname{argmax}_c (Rbf(z, c)) \quad (3)$$

Where:

- $c$  : any neuron of the map,
- $w_c$  : the mean vector associated to the neuron  $c$ ,
- $w_{c[i]}$  : the  $i^{\text{th}}$  component of the vector  $w_c$ ,
- $\sigma_c$  : the variance of the neuron  $c$ ,
- $z$  : the observation vector presented to the map input,
- $z[i]$  : the  $i^{\text{th}}$  component of the vector  $z$ ,
- $g$  : the winning neuron of the vector  $z$ ,
- $n$  : the dimension of the observation space, in our case  $n=5$ .

*Adaptation phase:* To proceed to the calculation of the parameters average and variance of every neuron  $c$  of the map, PRSOM consider every observation of the training set. Several heaps are incremented by the impact of every observation:

-Values of each vector component of the input observation are first treated separately. The tie of neighborhood that binds the winning neuron to the neuron  $c$  that we want to modify, ponders them, and then they are added in zones of separated heaps. These heaps are destined to the calculation of the different components of the mean vector of the neuron  $c$  (equation 5).

-The quadratic distance heap between the observation  $z$  and its winning neuron, weighted by the neighborhood, is destined to the calculation of the variance of the neuron  $c$ .

$$\sigma_c = \sqrt{\frac{\sum_z \left[ K_{h(t)}(\delta(c, \chi(z))) * \sum_{i=1}^n (z[i] - w_{\chi(z)[i]})^2 \right]}{\left[ \sum_z K_{h(t)}(\delta(c, \chi(z))) \right]^n}} \quad (6)$$

Where:

- $c$  : the neuron to modify
- $g$  : the winning neuron of the influential observation
- $h^{(t)}$  : the temperature of the  $t$  cycle
- $K^{h(t)}$  : the function of neighborhood to the  $t$  cycle
- $\delta(g, c)$  : the topological distance between the neuron  $c$  to modify and the winning neuron  $g$
- $w_c$  : the mean vector associated to the neuron  $c$
- $\sigma_c$  : the variance of the neuron  $c$

function in the affectation process which we have called *Rbf* (for *Radial-bias function*) in equations (2) and (3). A neuron being provided of an average and a variance, we can calculate the value of the activation provoked by the observation in the normal law of the neuron (equation 2). The winner neuron is the one for which this activation is the strongest (equation 3).

-The heap of neighborhood relations is used to normalize the calculation of the different components of the mean vector, as well as the calculation of the variance (equation 6).

These values are not modified in an adaptive way all along the treatment, as the SOM fact. To each end of cycle, PRSOM calculates the average and the variance of every neuron globally so that its associated normal law regains the mixture of densities defined by itself and its neighbors. The influence zone around a neuron depends on the topological distance. The importance of the contribution brought by an observation depends on a function of neighborhood that is a kernel function  $K$  similar to the function of neighborhood used in SOM. The metrics used to establish the distance between two neurons is the topological distance that is to say the difference between indexes permitting to situate the neurons on the map. In the implementation, we used a very simplified function of neighborhood that is given by equation (4). We ponder by this function of neighborhood the contribution of the observation to the calculation of the mean and variance of the neuron according to the equations (5) and (6).

$$K_{h(t)}(\delta(c, g)) = \exp \left[ -0,5 * \frac{\delta(c, g)}{h(t)} \right] \quad (4)$$

$$w_c = \frac{\sum_z (K_{h(t)}(\delta(c, \chi(z))) * z[i])}{\sum_z K_{h(t)}(\delta(c; \chi(z)))} \quad (5)$$

### C. Learning and processing

The data of wells DF02 and DF03 are normalised between -1 and +1 (fig. 2). Then vectors corresponding to the 5 log measures: RHOB, PEF, NPHI, GR and DT are all presented (fig. 1) to the SOM algorithm. We use also log's data from the well DF02 as a learning base for training the map and then, we reuse the network, obtained in 200 cycles, with log's data from well DF03. Then the PRSOM algorithm considers this map.

Initially, averages are maintained constant to allow every neuron to value its variance. Then, every neuron is provided of a normal law. As shown in fig. 8, 40 cycles are sufficient for the quantification error stabilization (see next section). Then, averages are freed in order to allow a simultaneous updating of variances and averages. One thousand cycles are

launched with a very weak temperature, varying from 3 to 1 so that to disturb the least possible the map structure. Table III presents the classifier performances according to the map size and the used algorithm. We divided the training set into 3 groups:

- Observations that correspond to zones of underground cores. We have for these data the exact class that it is necessary to get. We will call these 503 data "Core Set".
- Observations that correspond to a zone for which the expert provided an approximation of rock classes composing the faciès. We will call "Expert Set" the totality of these 742 data. The Expert Set only concerns the DF02 well.

- Well logging measures for which we didn't have cores, nor evaluation of the expert. We cannot provide any quantitative appreciation of results for these data.

Table III contains 3 columns: SOM, PRSOM V (update variances with constant averages) and PRSOM V+M (Simultaneous updating of variances and averages). We see that the only variance establishment does not modify greatly the results. On the other hand modifications brought by the simultaneous updating of averages and variances are important. We note that the PRSOM algorithm almost always improves topological map performances developed by the SOM algorithm.

- 1) Evaluate the temperature  $h$  of the cycle according to the equation 1
- 2) for every observation  $z$  of the training set :
  - present the observation  $z$  to the classifier,
  - calculate the value of the activation produced in the function of density of every neuron  $c$ , according to the equation 2,
  - choose the winning neuron  $g$  according to the equation 3,
  - read the following observation.
- 3) at the end of the cycle :
  - For every neuron  $c$  of the map :
  - For every observation  $z$  of the training set :
    - establish the topological distance  $\delta(c, g)$  between the neuron  $c$  and the winning neuron  $g$  of this observation  $z$ ,
    - evaluate the neighborhood between the winning neuron  $g$  and the neuron  $c$ , (equation 4),
    - add the contribution of the observation  $z$  to heaps constituting numerators and denominators of equations 5 and 6,
  - Calculate the mean vector of the neuron  $c$ , according to the equation 5.
  - Calculate the variance of the neuron  $c$ , according to the equation 6.
- 4) Return to 1 until to have done all cycles wanted.

Table II. The PRSOM algorithm

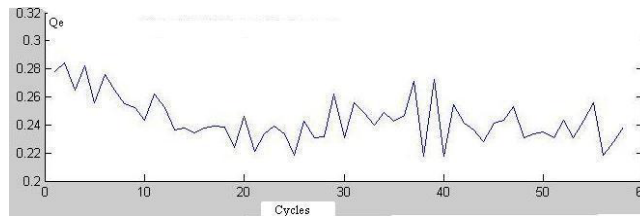


Fig. 8. PRSOM quantitative error  $Q_e$

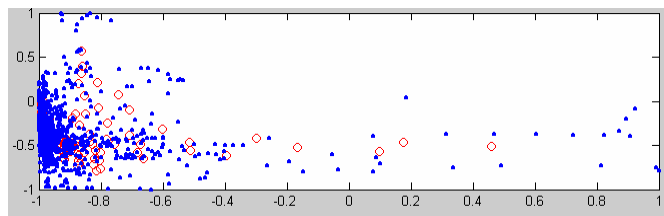


Fig. 9. Neurons on the map (o) and corresponding input data vectors (\*)

Table III. Improvement of performances by PRSOM algorithm

Size of the map	Percentage of error number over the Core set (%) 503 observations			Percentage of error number over the (Core + Expert) set (%) 1245 observations			Total number of neurons	Number of used neurons
	SOM	PRSOM V	PRSOM V+M	SOM	PRSOM V	PRSOM V+M		
13x7	14,54	13,34	10,21	32,77	34,66	29,88	91	91
20x7	11,46	13,34	11,08	36,54	35,52	30,69	140	138
17x5	12,29	11,38	08,78	36,72	35,83	25,89	85	85
10x10	13,58	12,76	09,71	37,28	35,64	30,42	100	100
20x20	07,93	08,68	05,29	33,39	28,34	26,55	400	350
25x25	05,28	05,96	02,68	28,45	24,88	19,77	625	515

#### D. The numeric criteria

Table 3 shows the method performances by considering "qualitative" errors i.e. by considering the geological aspect of the obtained lithofacies. Here, we measure the PRSOM performances by considering "quantitative" errors. We evaluate the quality of the training through a criteria that we called "quantification error" ( $Q_e$ ) that permits to appreciate the quality of regroupings. It is about the root squared of intra-class variance. The calculation of the  $Q_e$  measures the distance between neurons of the map and observations that they represent (equation 7). The reduction of  $Q_e$  gives account of the neuron adaptation to partitions that they defined. Figure 8 shows that  $Q_e$  begins to stabilize from 40 cycles, we have the certainty that the learning process is correctly performed. We stop the execution of PRSOM if  $Q_e$  stabilizes completely or if the maximum number of cycles is reached.

$$Q_e = \sqrt{\frac{\sum_z \sum_i (z[i] - w_{g[i]})^2}{N}} \quad (7)$$

Where:

- $z$  : any observation of the training set,
- $g$  : the winning neuron for the  $z$  observation,
- $w_g$  : the weight vector associated to the winning neuron  $g$ ,
- $w_g [i]$  : the  $i^{\text{th}}$  component of the vector  $w_g$ ,
- $N$  : the number of observations forming the training set.

#### E. Convergence proof

During the execution of the algorithm we obtain a sequence of weight sets  $W^0, W^1, \dots, W^t, \dots$  and a sequence of variance sets  $\sigma^1, \dots, \sigma^t, \dots$  such that for all  $t$  iteration, the cost function  $E$  verifies ([6], [12]) :

$$E(\chi^t, W^t, \sigma^t) \leq E(\chi^{t-1}, W^{t-1}, \sigma^{t-1})$$

The competition phase (or affectation phase) is executed by using the affectation function  $\chi$  (equation 3). The *argmax* function returns the index  $c$  for which the probability is the highest. Then, we obtain the inequality:  $E(\chi^t, W^t, \sigma^t) \leq E(\chi^{t-1}, W^{t-1}, \sigma^{t-1})$ . The adaptation phase (or minimisation phase) is executed by using the steepest descent method which allows to obtain the inequality :  $E(\chi^{t-1}, W^t, \sigma^t) \leq E(\chi^{t-1}, W^{t-1}, \sigma^{t-1})$ . Since the function  $E(\chi, W, \sigma)$  decreases at each iteration, the algorithm

converges in a limited number of iterations. The stationary point is a local minimum of  $E(\chi, W, \sigma)$ .

## VI. RESULTS AND INTERPRETATION

In order to have a best idea of expected results, an expert provided us within sight of the logfacies an estimate of the types of rocks awaited for part of well DF03. The expert reads the curves of the measurements to evaluate the class of corresponding rocks. This correspondence is not always very well defined, so that we have sometimes up to 4 possible cases for the estimate of only one point of well. It is thus possible for the expert to provide "precise" limits between the various benches of rock. These limits are sometimes evaluated with a margin of a few meters. These estimates having been proposed starting from the reading of the logfacies, they do not bring same information as the underground cores. For this reason, expert knowledge can be erroneous; it does not make it possible to determine in a very fine way the changes of rock when the layers are very thin. However, with these estimates, it will be possible to quantify the performances of our classifier: figure 8 shows that the PRSOM quantitative error  $Q_e$  stabilizes between 0,22 and 0.26 from 40 cycles, figure 5 and 9 shows that the neurons represent well the input data space. We present the lithofacies of wells DF02 and DF03 obtained using the SOM method (figures 6 and 7 respectively) and lithofacies obtained using the PRSOM method (figures 10 et 11 respectively). We can do two notices:

- The upper triassic (2825-2890 meters) is composed essentially of evaporite rocks (salt, anhydrite, dolomitic marl, marly limestone...) separated by banks of dolomitic clayey, fine to coarse clayey and coarse sandstone. The lower triassic (2890-2955 m) is composed essentially of red and green clay and argillite, quartzite and quartzite sandstone and clay-sandstone separated by micaceous fine sandstone, chalky sand and dolomitic clayey. This resulting description, well illustrated either in figures 7 and 8 or figures 11 and 12, is closed enough to the global model of wells that are available in the studied zone in the south of Algeria and susceptible to contain hydrocarbons ([2],[3]).
- We have obtained finest prediction with the PRSOM method.

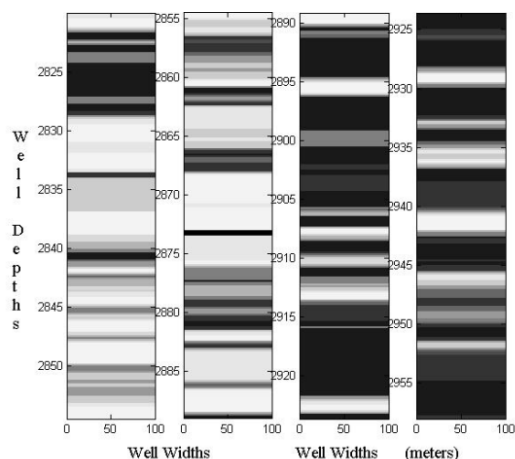


Figure 10. Lithofacies obtained for DF02 by PRSOM method

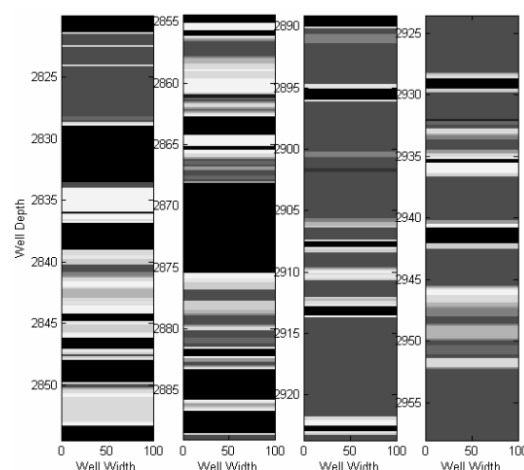


Figure 11. Lithofacies obtained for DF03 by PRSOM method

## VII. CONCLUSION

The lithology controls the strategies for reservoir management and it is with porosity the primary key to make a reliable reservoir model. Neural network analysis is one of the latest technologies available to the petroleum industry [4]. The proposed method enhanced the performance of the geology expert to find quickly the lithology of a given well. Then, many studies and analysis (lateral reservoir characterization, rocks porosity, permeability, reservoir volume, hydrocarbon distribution...) will be simplified. Using SOM method and PRSOM combined with radial bias functions neural network technique; we have successfully estimated the lithology of well DF02 and DF03. The PRSOM neural network using data from 3 wells (DF01, DF02 and DF03) provided a better and finest identification. Indeed, layers of rocks found in facies of figure 10 and 11 are thinner than those found in facies of figure 6 and 7. Some points as log's selection and expert interaction may be improved. We also need some precise information about the exact situation of the wells. The results described here open the field of neural research for log's data's study, generalization of neural networks to a drilling field and, why not, construction of an universal classification tool. We also think that if we quantitatively combine seismic and well log data with stratigraphical information ([1], [19]) we would generate reliable lithology and rock-property models. It is also interesting to consider the uncertainty [13] related to such earth science applications by using neural-fuzzy ([22], [27]), rule based ([17] [25]), or fuzzy-ARTMAP [28]

## REFERENCES

[1] O. E. Adegbenga, "High resolution sequence stratigraphic and reservoir characterization studies of D-07, D-08 and E-01 Sands, Block 2 Meren Field, Offshore Niger Delta," in *AAPG Conference and Exhibition*, September 21-24, 2003. Barcelona, Spain.  
[2] H. Aider, "Contribution des diagraphies différées à l'évaluation de paramètres des réservoirs," *Second scientific and technical days of the Sonatrach*, Algiers April 21-24, 1996 pp 115-130.

[3] M. Aliev, et al, "Structures géologiques et perspectives en pétrole et en gaz du Sahara Algérien," *Sonatrach éditions Algiers*. (1971).  
[4] F. Aminzadeh, "Challenging Problems in the Oil Industry and applications of AI and Soft Computing," in *Int. Joint Conf. on Artificial Intelligence IJCAI*, Mexico, Aug. 9-15, (2003).  
[5] F. Aminzadeh, J. Barhen, C.W. Glover, and N.B. Toomarian, "Reservoir parameter estimation using hybrid neural network," in *Computers & Geosciences*, vol. 26, pp. 869-875. (2000).  
[6] F. Anouar, "Modélisation probabiliste des cartes auto-organisées. Application en classification et en régression," in *PhD Thesis (Chapter 3)* National conservatory of arts and professions CNAM Paris V. (1996).  
[7] K Baddari, and A.A. Nikitin, "Statistical processing of geophysical data," *The second scientific and technical days of the Sonatrach*, Algiers April 21-24 pp 205-220. (1996).  
[8] M. Barbaroux, et al., "Generalized Fractal Dimensions: Equivalences and Basic Properties," in *Journal de Mathématiques Pures et Appliquées*, Sept. (2000).  
[9] L. Bougrain, and F. Alexandre, "Unsupervised connectionist algorithms for clustering an environmental data set: A comparison.," in *Neurocomputing* Vol 28 pp 177-189. (1999)  
[10] G. A. Carpenter, and S. Grossberg, "Adaptive resonance theory," in *The Handbook of Brain Theory and Neural Networks*, 2nd ed., Michael A. Arbib, Editor, Cambridge, Massachusetts: MIT Press. (2002)  
[11] H. Chang, et al., "Lithofacies identification using multiple adaptive resonance theory neural networks and group decision expert system," in *Computers & Geosciences* 26 pp 591-601. (2000)  
[12] S. Chikhi, and H. Shout, "Using probabilistic neural networks to construct well facies," in *WSEAS Transactions on Systems*, Issue 4 Vol. 2, pp 839-843. (2003)  
[13] C. S. Claude, "Practical Analysis for Reservoir Uncertainty. In AAPG (American Association of Petroleum Geologists) Conference and Exhibition, September 21-24, Barcelona, Spain. (2003)  
[14] K. Derguini, "Applications Sédimentologiques des Diagraphies," in *The Algerian Geology Journal*. pp 1-29. (1995)  
[15] C. Dreyfus, et al., "Réseaux de neurones. Méthodologie et applications," in *Eyrolles éditions*, Paris. (2002)  
[16] D. Frayssinet, "Utilisation des réseaux de neurones en traitement des données de diagraphies: prédiction et reconstitution de faciès lithologiques," *Master thesis*. National conservatory of arts and professions C.N.A.M. Paris V. (2000)  
[17] T. D. Gedeon, H. Kuo, and P. M. Wong, "Rule Extraction Using Fuzzy Clustering for a Sedimentary Rock Data Set," in *International Journal of Fuzzy Systems*, Vol. 4, No. 1, pp 600-605. (2002)  
[18] S. Gottlib-Zeh, L. Briquieu, and A. Veillerette, "Indexed Self-Organization Map: a new calibration system for a geological interpretation of logs," *Proceedings of IAMG'99*, VI, pp 183-188. Lippard, Naess and Sinding-Larsen Editons Norway. (1999)